

Focused ion beam post-processing of optical fiber Fabry-Perot cavities for sensing applications

Ricardo M. André,^{1,2,*} Simon Pevec,³ Martin Becker,² Jan Dellith,² Manfred Rothhardt,² Manuel B. Marques,¹ Denis Donlagic,³ Hartmut Bartelt,² and Orlando Frazão¹

¹INESC Porto and Department of Physics and Astronomy, Faculty of Sciences, University of Porto, Rua do Campo Alegre 687, 4150-179 Porto, Portugal

²Leibniz Institute of Photonic Technology (IPHT Jena), Albert-Einstein-Straße 9, 07745 Jena, Germany

³Faculty of Electrical Engineering and Computer Science, University of Maribor, 2000 Maribor, Slovenia

randre@inescporto.pt

Abstract: Focused ion beam technology is combined with chemical etching of specifically designed fibers to create Fabry-Perot interferometers. Hydrofluoric acid is used to etch special fibers and create microwires with diameters of 15 µm. These microwires are then milled with a focused ion beam to create two different structures: an indented Fabry-Perot structure and a cantilever Fabry-Perot structure that are characterized in terms of temperature. The cantilever structure is also sensitive to vibrations and is capable of measuring frequencies in the range 1 Hz – 40 kHz.

©2014 Optical Society of America

OCIS codes: (060.2310) Fiber optics; (060.2370) Fiber optics sensors; (230.4000) Microstructure fabrication; (050.2230) Fabry-Perot; (160.2290) Fiber materials.

References and links

1. S. Reyntjens and R. Puers, "A review of focused ion beam applications in microsystem technology," *J. Micromech. Microeng.* **11**(4), 287–300 (2001).
2. A. A. Tseng, "Recent developments in micromilling using focused ion beam technology," *J. Micromech. Microeng.* **14**(4), R15–R34 (2004).
3. C. Martelli, P. Olivero, J. Canning, N. Groothoff, S. Prawer, S. Huntington, and B. Gibson, "Micromachining long period gratings in optical fibres using focused ion beam," in *Bragg Gratings, Photosensitivity, and Poling in Glass Waveguides* (Optical Society of America, 2007), p. BTuC6.
4. J.-L. Kou, S.-J. Qiu, F. Xu, Y.-Q. Lu, Y. Yuan, and G. Zhao, "Miniaturized metal-dielectric-hybrid fiber tip grating for refractive index sensing," *IEEE Photon. Technol. Lett.* **23**(22), 1712–1714 (2011).
5. J. L. Kou, S. J. Qiu, F. Xu, and Y. Q. Lu, "Demonstration of a compact temperature sensor based on first-order Bragg grating in a tapered fiber probe," *Opt. Express* **19**(19), 18452–18457 (2011).
6. D. Iannuzzi, K. Heeck, M. Slaman, S. de Man, J. H. Rector, H. Schreuders, J. W. Berenschot, V. J. Gadgil, R. G. P. Sanders, M. C. Elwenspoek, and S. Deladi, "Fibre-top cantilevers: design, fabrication and applications," *Meas. Sci. Technol.* **18**(10), 3247–3252 (2007).
7. K. P. Nayak, F. Le Kien, Y. Kawai, K. Hakuta, K. Nakajima, H. T. Miyazaki, and Y. Sugimoto, "Cavity formation on an optical nanofiber using focused ion beam milling technique," *Opt. Express* **19**(15), 14040–14050 (2011).
8. F. Wang, W. Yuan, O. Hansen, and O. Bang, "Selective filling of photonic crystal fibers using focused ion beam milled microchannels," *Opt. Express* **19**(18), 17585–17590 (2011).
9. J. L. Kou, J. Feng, Q. J. Wang, F. Xu, and Y. Q. Lu, "Microfiber-probe-based ultrasmall interferometric sensor," *Opt. Lett.* **35**(13), 2308–2310 (2010).
10. J. L. Kou, J. Feng, L. Ye, F. Xu, and Y. Q. Lu, "Miniaturized fiber taper reflective interferometer for high temperature measurement," *Opt. Express* **18**(13), 14245–14250 (2010).
11. W. Yuan, F. Wang, A. Savenko, D. H. Petersen, and O. Bang, "Note: Optical fiber milled by focused ion beam and its application for Fabry-Pérot refractive index sensor," *Rev. Sci. Instrum.* **82**(7), 076103 (2011).
12. S. Pevec, E. Cibula, B. Lenardic, and D. Donlagic, "Micromachining of optical fibers using selective etching based on phosphorus pentoxide doping," *IEEE Photon. J.* **3**(4), 627–632 (2011).
13. S. Pevec and D. Donlagic, "All-fiber, long-active-length Fabry-Perot strain sensor," *Opt. Express* **19**(16), 15641–15651 (2011).
14. S. Pevec and D. Donlagic, "Miniature micro-wire based optical fiber-field access device," *Opt. Express* **20**(25), 27874–27887 (2012).

-
15. T. Wei, Y. Han, H.-L. Tsai, and H. Xiao, "Miniaturized fiber inline Fabry-Perot interferometer fabricated with a femtosecond laser," *Opt. Lett.* **33**(6), 536–538 (2008).
 16. L. Zhao, L. Jiang, S. Wang, H. Xiao, Y. Lu, and H.-L. Tsai, "A high-quality Mach-Zehnder interferometer fiber sensor by femtosecond laser one-step processing," *Sensors* **11**(1), 54–61 (2011).
 17. L. Yuan, T. Wei, Q. Han, H. Wang, J. Huang, L. Jiang, and H. Xiao, "Fiber inline Michelson interferometer fabricated by a femtosecond laser," *Opt. Lett.* **37**(21), 4489–4491 (2012).
 18. J. Kalenik and R. Pajak, "A cantilever optical-fiber accelerometer," *Sens. Actuators A Phys.* **68**(1-3), 350–355 (1998).
-

1. Introduction

Focused Ion Beam (FIB) is a commercially available technology developed for, and mainly employed by, the semiconductor industry. FIB systems are very similar to Scanning Electron Microscopes (SEM), but instead of an electron beam they use an ion beam, generally of gallium ions (Ga^+) [1]. They can be operated with small currents for imaging just like the SEM systems, or with higher currents for milling and sputtering. Modern systems include both an ion beam column and an electron beam column (dual-beam systems), which allow for a higher flexibility in imaging/milling the substrate [2].

In the last few years, FIB technology has been applied to optical fibers, leading to new and interesting ways of creating very small and short optical fiber devices. FIB has been combined with optical fiber technology to create structures ranging from long-period [3] and fiber Bragg gratings for refractive index [4] and temperature [5] sensing to more complex structures such as fiber-top cantilevers for very small displacement sensing [6]. Nanofiber cavities have been fabricated by milling two FBGs on a nanofiber with FIB [7]. FIB has also been used for the milling of channels in microstructured optical fibers, thus allowing for selective filling of these fibers [8]. Fabry-Perot (FP) cavities have also been fabricated using FIB. Most are created on tapered fiber tips in order to reduce the required FIB milling [9–11] to a minimum. One downside of FIB processing is the time it takes to mill large quantities of material. This is why, in the vast majority of the works involving FIB processing of optical fiber, another, faster technique is used to somehow reduce the amount of material to be milled. The most common method is tapering, either by creating nanofibers or tapered fiber tips.

In our effort, another technique is used instead of tapering: hydrofluoric acid etching of specifically designed fibers [12]. This allows for the creation of microwires and thus reduces the FIB milling time necessary to create a structure. This paper reports about two different sensing FP structures milled with FIB. The FP structures were milled on 15 μm -diameter microwires. One of the structures is a simple FP cavity created by milling an indentation in the microwire. This structure was characterized as a high temperature sensor. The other structure is a microwire cantilever FP structure and was characterized as a temperature and vibration sensor.

2. Fabrication

The fabrication of the Fabry-Perot structures can be divided into two steps: the fabrication of the microwire by chemical etching micromachining, and the milling of a gap in the microwire with focused ion beam technology. This two-step process allows for the much faster fabrication of microstructures than using solely FIB on standard fiber. Accessing the light guiding region with FIB would take too long on a standard fiber, and the structures would be very poorly defined, due to the high aspect ratio necessary.

2.1 Microwire fabrication with chemical etching

This micromachining technique is based on the much higher etching rate of phosphorus pentoxide-doped silica when compared to pure silica. This way, structure forming fibers can be engineered with pure silica regions and P_2O_5 -doped regions so that, after etching, only the pure silica regions remain, leaving just the desired microstructure [13,14]. This technique is

used to create microwires which are then further post-processed using FIB technology. After splicing the structure forming fibers (SFF) to a single-mode fiber (SMF), the SFF is cleaved to the desired length (see Figs. 1(a)–1(f)). To prevent etching from the top of the fiber, an additional short section of a coreless all-silica multimode fiber (cMMF) is spliced to the top of the SFF. The structure forming fiber was cleaved using an ultrasonic YORK FK 11 cleaver set at a tensile strength of 2 N. The splicing was performed by a filament fusion splicer (Vytran FFS 2000) that led to splices with losses below 0.2 dB [14].

The whole structure is then placed inside a HF solution with 40% concentration. Initially only pure silica is in contact with the solution and, consequently, the whole structure is etched uniformly, but when the outer silica shell is etched away and the acid comes into contact with the doped region, preferential etching of the P_2O_5 -doped silica occurs. The P_2O_5 concentration of the SFF is about 8.5 mol % which means that the etching rate of the P_2O_5 -doped region is about 30 times higher than the etching rate of pure silica. Etching in 40% HF at room temperature ($\sim 25^\circ C$), with no stirring leads to etching rates of 1 $\mu m/min$ for pure silica and 31 $\mu m/min$ for the P_2O_5 -doped region. The process was concluded by rinsing the structures in distilled water. The total etching times depend on the desired microwire diameter and the external temperature, and can range from 15 to 20 minutes. The structure that remains after chemical etching consists of a microwire with a diameter of 15 μm , aligned with the single-mode lead-in fiber core and two side support beams that, due to the complete misalignment with the SMF core, do not guide light (see Fig. 1(f)). These side support beams give the microwire protection and help the whole structure retain its form. Even though the microwire, when in air, supports several modes after being etching, practically only one mode is launched by the SMF in the current configuration. This required special care in structure design as described in detail in [14]. The guiding losses for the microwires are below 0.4 dB for diameters of 15 μm .

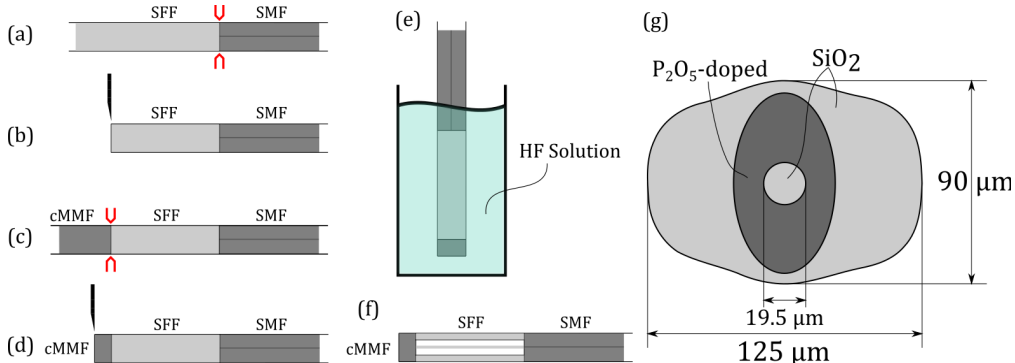


Fig. 1. Microwire fabrication process: (a) SMF-SFF fusion splicing; (b) cleaving to desired length; (c) SFF-cMMF fusion splicing; (d) cMMF cleaving (30-40 μm); (e) etching; (f) final structure; (g) SEM micrograph of etched microwire; (h) structure forming fiber cross-section.

2.2 Cavity fabrication with focused ion beam

After the microwire is created, a focused ion beam is used to mill the microwire and create two different Fabry-Perot structures. Before FIB milling, the microwires were sputter-coated with a thin tantalum film (ca. 50 nm). This is necessary to avoid charging during electron beam and ion beam operation of the fiber, as silica is non-conductive. The charging will affect the milling because it will cause the ion beam to drift from its intended spot position, effectively reducing the resolution and quality of the milled structures. In the milling of these structures an ion current of approximately 1 nA is used for a primary coarse milling of the cavities. After this, a polishing is performed using a much smaller current of 100-300 pA. The currents were adjusted so that the primary milling times did not exceed one hour and the secondary polishing times did not exceed 20 min to avoid charging and consequent drift

effects. The surface quality is rough after the primary milling due to the high current employed and also due to the redeposition of some of the milled material but, after the polishing, the surface roughness greatly decreases. Flat, parallel walls can be obtained because the aspect ratio of the milled structure is not high [2]. The first structure milled consists of an indentation in the microwire (see Fig. 2, top). The reflections at both silica-to-air interfaces (signaled in Fig. 2 top) result in a low-finesse FP cavity. The cavity has a length of approximately 167 μm .

The second structure is similar save that a whole section of the microwire is removed instead of just a half cylinder section (see Fig. 2 bottom). This results in a completely cleaved microwire that is suspended from the fiber-top side. The microwire stays in place due to the side support beams that still remain after the milling process. This structure also behaves as a FP cavity, being that the reflecting interfaces are the fiber top and the silica-to-air interface at the air gap signaled in Fig. 2 bottom. In this case, the cavity has a much greater length of approx. 1025 μm .

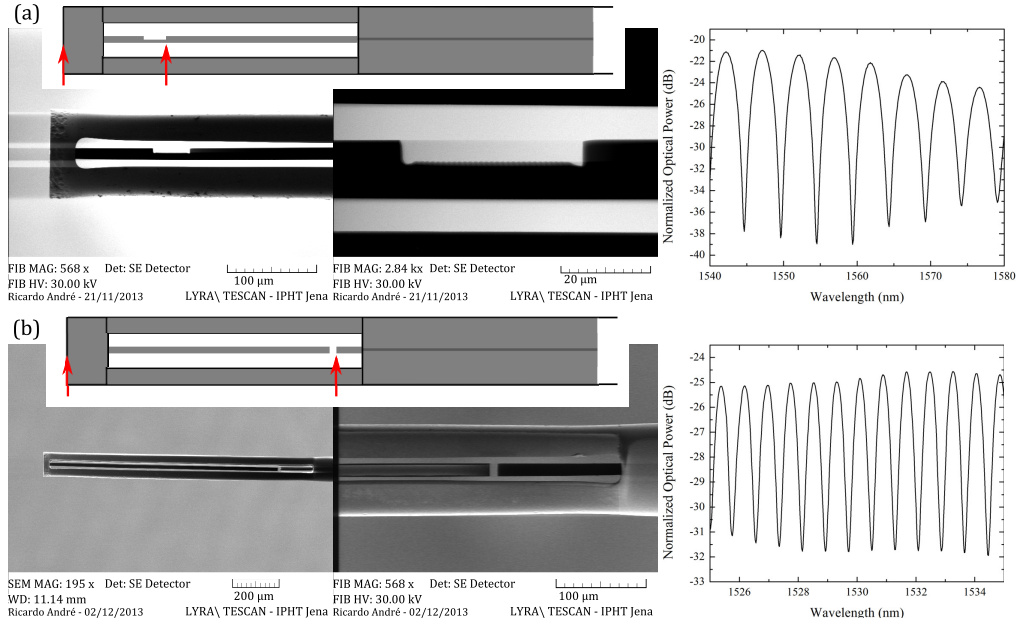


Fig. 2. Indented Fabry-Perot cavity SEM micrographs and related optical reflection spectrum (top); cantilever FP structure micrograph and related optical reflection spectrum (bottom).

3. Results

3.1 Optical spectra

The Fabry-Perot structures were analyzed in a simple reflection setup consisting of an optically amplified spontaneous emission (ASE) broadband source @ 1550 nm, an optical circulator, and an optical spectrum analyzer. The resulting optical spectra of both structures after focused ion beam milling show a channeled spectrum typical of a low finesse FP structure, but they have completely different fringe spacings, as the cavity lengths are different (see Fig. 2). Estimating the cavity length using the fringe spacing can provide a better understanding of where the reflections are taking place. The following expression can easily be derived from the resonance wavelength expression for a FP cavity, taking into account two consecutive resonant wavelengths λ_1 and λ_2 :

$$L = \frac{\lambda_1 \lambda_2}{2 \cdot n_{eff} \cdot \Delta\lambda} \quad (1)$$

Using values obtained from the reflection spectra one obtains lengths of approximately 172 μm and 1026 μm for indented FP and cantilever FP structures, respectively. Comparing these lengths with the SEM micrographs one readily identifies that the fringes come from reflections at the fiber top and at the first interface of the milled section (both signaled in Fig. 2). The lengths measured from the SEM micrographs for these two structures are 167 μm and 1025 μm , which are in good accordance, given the uncertainty of measuring the SEM micrographs.

3.2 Temperature

For temperature characterization, the Fabry-Perot structures were placed inside a tubular oven, and the temperature was varied from 100 to 550 $^{\circ}C$. An optical spectrum analyzer with a resolution of 1 pm was used to acquire the spectra. The wavelengths were tracked using MATLAB® to determine the spectral shift. For each temperature measurement, the system (oven + sensor) is stabilized at each temperature point for approximately 2 minutes to ensure a stable and uniform temperature in the oven. Both structures present a similar, slightly quadratic behavior, but two linear regimes can be defined (see Fig. 3). For low temperatures (100-300 $^{\circ}C$), sensitivities of 11.5 pm/K and 12.3 pm/K were obtained for indented FP and cantilever FP, respectively. For higher temperatures (300-550 $^{\circ}C$), 14.2 pm/K and 15.5 pm/K were obtained for indented FP cavity and cantilever, respectively. These results are in accordance with the only other paper that FP cavities in optical fiber milled with FIB [10]. Kou et al. milled a FP cavity on a tapered fiber tip and obtained a temperature response given by a third order polynomial with an average sensitivity of 17 pm/K, similar to the sensitivities obtained in this work [10]. When considering structures milled with femtosecond laser micromachining, sensitivities in a wide range have been obtained from nearly insensitive structures (0.074 pm/K [15]) to highly sensitive ones (51.5 pm/K [16]). Structures with a similar sensitivity (14.7 pm/K [17]) have been reported.

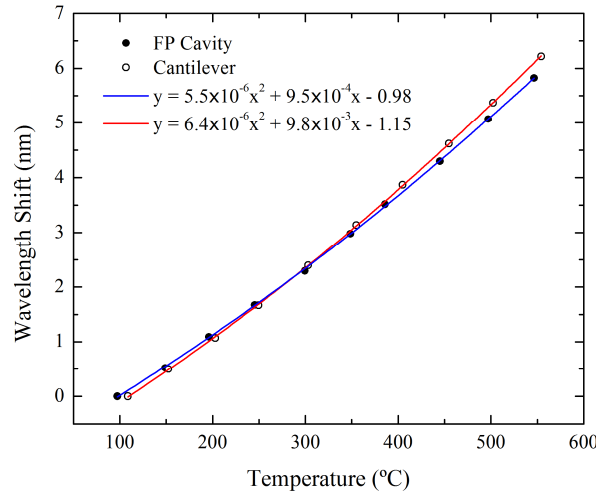


Fig. 3. Temperature response of both Fabry-Perot structures: indented FP cavity (full dots, blue line) and FP cantilever structure (hollow dots, red line).

3.3 Vibration

In the cantilever Fabry-Perot structure, the microwire is solely suspended by one of its ends as opposed to the indented FP structure where both ends of the microwire are fixed. This

suspended microwire has freedom to move relative to the bulk input fiber, allowing for aligned and misaligned positions. Using this property, it is possible to apply this structure as a vibration sensor. The structure was attached to an acoustic vibrating system that produced a vibration frequency in the range from 1 Hz to 40 kHz. A tunable laser set at 1561 nm was used instead of the ASE source, and the optical spectrum analyzer was replaced by a photodiode so that the power at a specific wavelength could be monitored. This would make the cantilever effectively work as an intensity sensor, obtaining maximum intensity when the microwire is aligned and minimum intensity when it is misaligned. In Fig. 4, three different signals taken directly from the photodiode for three different frequencies applied (90 Hz, 1.2 kHz and 14 kHz) are shown. Using these signals it is possible, by taking their Fast Fourier Transforms (FFTs), to determine the applied frequencies in each case. Using this simple setup, the peak corresponding to the applied frequency was identifiable in the whole range (1 Hz – 40 kHz). Here the top limit of this range was limited by the maximum frequency generated by the vibration system and not by the FP structure itself. It is possible to estimate the first resonance frequency of the cantilever, that would ultimately limit the working range of the device, using the following equation derived from the equation of motion for a cylindrical beam [18]:

$$f_1 = \frac{3.52}{2\pi l^2} \sqrt{\frac{EI}{\rho A}} = \frac{1.76a}{2\pi l^2} \sqrt{\frac{E}{\rho}} \quad (2)$$

where E is Young's modulus of elasticity, ρ is the mass density, I is the second moment of area, A is the cross-sectional area of the beam, l is the beam length and a its radius. Typical values for silica fibers are $E = 7.2 \times 10^{10}$ N/m² and $\rho = 2.2$ kg/m³. For this cantilever one has: $a = 7.5$ μm and $l = 1025$ μm. This yields an estimated resonance frequency of 362 kHz, way above the working range tested in this work. Also present in the FFT spectra are the second and even third harmonics for some of the frequencies applied.

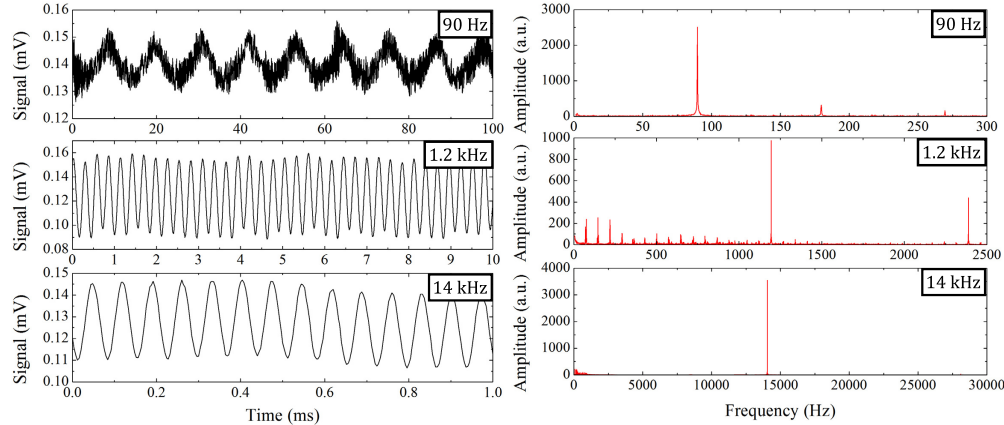


Fig. 4. Fabry-Perot cantilever structure: time responses (left) and related fast Fourier transforms (right) when an external frequency is applied.

4. Conclusions

In this work, the combination of chemical etching and micromachining of specially designed and doped fibers with focused ion beam milling was proposed and demonstrated. To the authors' knowledge, this is the first time that this has been attempted and achieved. Two different Fabry-Perot structures were generated by FIB milling of a microwire created by chemical etching. One consists of a milled indentation on the microwire while in the other, the microwire is totally cleaved and lies suspended on just one end, leaving it susceptible to

vibration. The initial fiber design allows for this because of the existence of side support beams that hold the microwire in place. This free-standing microwire is what allows this structure to work as a vibration sensor. Most fiber vibrations sensors are based on using two distinct fibers for input and output and an external system to hold them in place, using one fiber as a cantilever [18]. The sensor presented here has the advantage of being completely integrated in the fiber, with no need for external support structures. Temperature sensitivities from 11.5 to 15.5 pm/K were obtained for both the FIB milled FP structures when considering a temperature range from 100 to 550 °C. As for vibration, the cantilever system detects frequencies from 1 Hz to 40 kHz, and potentially as high as the first resonance frequency of 360 kHz.

This work showed that a FIB can be used for processes such as selective cleaving and creating simple structures that could not be achieved otherwise with such high optical quality. FIB can also be combined with other post-processing techniques to create new and novel optical sensors and devices opening doors for miniaturized and fiber-integrated elements.

Acknowledgments

This work was supported by the COST Action TD1001. The work of Ricardo André was supported in part by Fundação para a Ciência e Tecnologia under the grant SFRH/BD/84048/2012. This work was also partially funded by the Slovenian Research Agency (ARSS) program no. P2-0368. The P₂O₅-doped fibers used in this research were kindly produced and supplied by Optacore d.o.o., Slovenia.